

# Pseudogap Phase: Exchange Energy Driven vs. Kinetic Energy Driven

Zhengcheng Gu, Tao Li, and Zheng-Yu Weng

Center for Advanced Study, Tsinghua University, Beijing 100084, China

We show that *both* kinetic and superexchange energies of the  $t - J$  model may be read off from the optical data, based on an optical sum rule for the Hubbard model. Then we comparatively study two mean-field theories of pseudogap phase based on the  $t - J$  model. We find that while the pseudogap phase is superexchange-energy-driven in the slave-boson resonating-valence-bond (RVB) state, it is kinetic-energy-driven in the bosonic RVB state. The sharp contrast in the mechanisms of the pseudogap phases can be attributed to the fact that the antiferromagnetic (AF) correlations behave quite differently in two mean-field states, which in turn distinctly influence the kinetic energy of charge carriers. We elaborate this based on some detailed studies of the superexchange energy, kinetic energy, uniform spin susceptibility, equal-time spin correlations, dynamic spin susceptibility, as well as the optical conductivity. The results provide a consistent picture and understanding on two physically opposite origins of pseudogap phase. In comparison with experimental measurements, we are led to conclude that the pseudogap phase in the cuprates should be kinetic-energy-driven in nature.

PACS numbers: 74.20.Mn, 74.25.Gz, 74.25.Ha

## I. INTRODUCTION

The pseudogap phase is one of the most interesting and unconventional regimes observed in the underdoped cuprate superconductors. Such a phenomenon has been identified [1] in NMR, ARPES, neutron-scattering, transport, optical conductivity and other experiments, which are absent in the traditional BCS superconductivity. The physical origin of such a pseudogap state remains controversial, with the proposed ones ranging from the RVB pairing [2–4], the loss of the phase coherence in the superconducting order parameter [5, 6], preformed electron pairing [7], to the d-density-wave theory [8], etc. A good understanding of the essential physics involved in the pseudogap phase will be of great importance in searching for a sensible microscopic theory of the high- $T_c$  cuprates.

In this paper, we propose to study the detailed driving mechanisms behind the pseudogap phase. So far, different driving mechanisms for the superconducting condensation have been studied extensively in literature [9–17]. As to be shown in this work, the nature of a pseudogap phase can be also meaningfully clarified by identifying, both experimentally and theoretically, whether it is kinetic-energy-driven or potential-energy-driven. Specifically we shall focus ourselves on the pseudogap phases based on the  $t - J$  model. Such a model is composed of two terms:  $H_{t-J} = H_t + H_J$  (see Sec. II), where the kinetic term is denoted by  $H_t$  and the superexchange term by  $H_J$ . Then one can ask whether the pseudogap state, if exists, is mainly driven by  $H_t$  or  $H_J$ , and how different possible driving mechanisms can be probed and verified (falsified) by experimental measurements.

Firstly we shall establish a very general relationship between the optical conductivity and the kinetic and superexchange energies in the  $t - J$  model. An important but subtle difference between the kinetic terms of the  $t - J$  model and the Hubbard model will be carefully examined and distinguished. In a single-band Hubbard model, the optical sum rule is generally given by [18]

$$\int_0^\Lambda \sigma_1(\omega, T) d\omega = \frac{\pi a^2}{2V} \langle -H_K \rangle \quad (1)$$

where  $\sigma_1(\omega, T)$  is the real part of the optical conductivity and  $\Lambda$  is some high-energy cutoff (higher than the Hubbard-Mott gap). On the right-hand-side (rhs),  $H_K$  is the kinetic energy of the Hubbard model,  $a$  is the lattice constant, and  $V$  is the volume. In the case of the  $t - J$  model (*i.e.*, the large- $U$  Hubbard model), the kinetic energy  $\langle H_K \rangle$  can be replaced by  $\langle H_t \rangle$ , if  $\Lambda$  is taken as some characteristic energy cutoff  $\Omega$  below which *only* no-double-occupancy intraband transitions of charges are allowed. However, if  $\Lambda$  is taken to be larger such that to allow the transitions to doubly occupied states, then the rhs of Eq.(1) will include additional contribution beside  $\langle H_t \rangle$  from the kinetic energy of the Hubbard model, which, as we will show in Sec. II, is nothing but  $2 \langle H_J \rangle$ , twice of the superexchange energy of the  $t - J$  model!

Thus, by properly choosing the magnitudes of  $\Lambda$  and  $\Omega$ , respectively, the optical data can provide crucial information on *both* the kinetic energy and superexchange energy of the  $t - J$  model and be effectively used to deduce the driving mechanisms for both pseudogap and superconducting states. As to be discussed in Sec. II, the recent optical measurement results [19] in the cuprate  $Bi_2Sr_2CaCu_2O_8$  can be read off, based on the present analysis, as strong evidence in support of the kinetic-energy-driven mechanism for *both* superconducting and pseudogap phases.

Then we shall study two distinct pseudogap phases defined in different mean-field theories of the  $t-J$  model, *i.e.*, the slave-boson RVB [20, 21] and bosonic RVB (b-RVB) [22, 23] mean-field states, respectively, which will be introduced in Sec. III. Then, we show that the pseudogap phase in the slave-boson RVB state is superexchange-energy-driven, while it is kinetic-energy-driven in the b-RVB state. The underlying physics is then explored in a comparative way in Sec. IV.

A detailed study of the static and dynamic spin susceptibility functions in Sec. IV reveals how the AF correlations evolve between the pseudogap and “normal” phases. In the slave-boson RVB state, the AF correlations near  $(\pi, \pi)$  are intrinsically weak in the “normal” state and by opening the RVB gap to enter the pseudogap phase, the superexchange energy will be reduced, whereas the kinetic energy simultaneously gets increased. In contrast, the AF correlations near  $(\pi, \pi)$  are already quite strong in the “normal” state of the b-RVB state such that the kinetic energy is very frustrated. By going into the pseudogap phase, the kinetic energy will get improved with suppressing AF correlations, which simultaneously results in an increase of the superexchange energy. Thus, whether a pseudogap phase in the  $t-J$  model is kinetic-energy-driven or superexchange-energy-driven crucially depends on which one of the kinetic energy and AF correlations gets “released” from a “suppression” status in the “normal” state.

Experimentally, the superexchange energy of  $H_J$  will be related to the nearest-neighbor (NN) spin-spin correlations, which can be decided by the imaginary dynamic spin susceptibility  $\text{Im} \chi(\vec{q}, \omega)$ , measurable by an inelastic neutron-scattering measurement, through the following sum rule

$$\langle \vec{S}_i \cdot \vec{S}_j \rangle = \int \frac{d^2 \vec{q}}{(2\pi)^2} \int_0^\infty \frac{d\omega}{\pi} (1 + n(\omega)) \text{Im} \chi(\vec{q}, \omega) \cos(\vec{q} \cdot (\vec{r}_i - \vec{r}_j)) \quad (2)$$

where  $n(\omega) = 1/(e^{\beta\omega} - 1)$ . Previously, based on this relation, arguments for superexchange-energy-driven superconductivity have been made in literature based on the neutron-scattering measurements. In particular, the SO(5) theory suggests [11, 12] that the superconducting transition in the high- $T_c$  superconductors is driven by the superexchange energy gain as the so called  $\pi$ -resonance mode [24] opens a new channel for AF spin fluctuations in the superconducting state. But for both the slave-boson RVB and b-RVB theories of the  $t-J$  model, the superconductivity is always kinetic-energy-driven. The b-RVB theory goes further to predict that the pseudogap phase is also kinetic-energy-driven, in which the resonance-like peak observed in  $\text{Im} \chi(\vec{q}, \omega)$  by neutron-scattering [24–26] is not interpreted as an emergent new mode, rather it simply comes from the low-lying spin excitations in the “normal” state, which are pushed upwards to a *higher energy* and become sharpened in the pseudogap phase. In other words, if the “normal” state is “extrapolated” into zero temperature, strong AF correlations near  $\omega \sim 0$  or even an AF long-range order can appear as evidenced by the non-Korringa behavior of the NMR  $1/T_1 T$  both calculated (Sec. IV) and observed experimentally in the cuprates. Therefore, in combination with the aforementioned optical measurements, the experiments seem overall in favor of the mechanism of kinetic-energy-driven as the origin of the pseudogap phase.

In Sec. II, the optical sum rules for the Hubbard and  $t-J$  models are discussed and a comparison with experiment is made. In Sec. III, we introduce and discuss two pseudogap phases in the slave-boson RVB and b-RVB theories based on the  $t-J$  model, and in Sec. IV, we present a comparative study of the pseudogap phases in two RVB mean-field states. Finally a discussion and conclusions are given in Sec. V.

## II. OPTICAL SUM RULES IN THE HUBBARD AND $t-J$ MODELS

The Hubbard model is defined by

$$H_{\text{Hub}} \equiv H_K + H_U = -t \sum_{\langle ij \rangle \sigma} (c_{i\sigma}^\dagger c_{j\sigma} + h.c.) + U \sum_i n_{i\uparrow} n_{i\downarrow}.$$

In the large- $U$  limit, the Hubbard model can be reduced [27] to the  $t-J$  model in the low-energy subspace of no double occupancy. This is usually done by dividing the Hilbert space into the low-energy subspace of no double occupancy and the high-energy subspace with doubly occupied sites. In the large- $U$  limit, two subspaces are separated by a gap of order of  $U$ . Correspondingly, the Hamiltonian can be divided into intra-subspace and inter-subspace pieces. Introducing the projection operator  $P_L$  and  $P_H$  for the low-energy subspace and high-energy subspace, respectively, the Hubbard Hamiltonian can be written as

$$H_{\text{Hub}} = H_L + H_H + H_{mix}$$

in which

$$\begin{aligned}
H_L &= P_L H_K P_L \\
H_H &= P_H H_K P_H + H_U \\
H_{mix} &= P_L H_K P_H + P_H H_U P_L
\end{aligned}$$

are the terms in the low-energy subspace, high-energy subspace, and the subspace-mixing term, respectively. The subspace-mixing term can be removed by a canonical transformation  $e^{iS}$  [27]. To the first order of  $\frac{t}{U}$ , the transformed Hamiltonian in the low energy subspace is the standard  $t - J$  model

$$\begin{aligned}
(e^{iS} H_{\text{Hub}} e^{-iS})_L &= P_L H_K P_L + iP_L [S, H_{mix}] P_L \\
&\equiv H_{t-J}
\end{aligned}$$

where  $H_{t-J} = H_t + H_J$ , with the kinetic term  $H_t$  and the superexchange term  $H_J$  defined by

$$H_t = -t \sum_{\langle ij \rangle \sigma} \left( \hat{c}_{i\sigma}^\dagger \hat{c}_{j\sigma} + h.c. \right), \quad (3)$$

$$H_J = J \sum_{\langle ij \rangle} \left( \vec{S}_i \cdot \vec{S}_j - \frac{1}{4} n_i n_j \right), \quad (4)$$

where  $\hat{c}_{i\sigma} = (1 - n_{i-\sigma}) c_{i\sigma}$  (here  $n_{i\sigma} = c_{i\sigma}^\dagger c_{i\sigma}$ ),  $\vec{S}_i = \frac{1}{2} \sum_{\alpha\beta} c_{i\alpha}^\dagger (\vec{\sigma})_{\alpha\beta} c_{i\beta}$ , and  $n_i = \sum_{\sigma} n_{i\sigma}$ .

Under the above canonical transformation, the kinetic energy of the Hubbard model is transformed into

$$(e^{iS} H_K e^{-iS})_L = H_t + 2J \sum_{\langle i,j \rangle} \left( S_i \cdot S_j - \frac{1}{4} n_i n_j \right) \quad (5)$$

in the low-energy subspace to the first order of  $\frac{t}{U}$ . The potential energy of the Hubbard model transforms into

$$(e^{iS} H_U e^{-iS})_L = -J \sum_{\langle i,j \rangle} \left( S_i \cdot S_j - \frac{1}{4} n_i n_j \right) = -H_J$$

in the low-energy subspace to the same order. Note that the transformed form of  $H_U$  is still positive-definite.

From these formulas, we can explicitly see an important but subtle difference between the kinetic energy in the  $t - J$  model and that of the underlying Hubbard model. Note that  $H_t$  solely contributes to the charge response in the  $t - J$  model with  $H_J$  as charge neutral in the subspace of no double occupancy. According to Eq.(5), however, the *kinetic energy* of the Hubbard model includes not only the kinetic term  $H_t$  of the  $t - J$  model, but also an *additional* term, which happens to be twice of the superexchange term  $H_J$ . Namely, the “kinetic energy” term  $H_t$  in the  $t - J$  model does not represent the *whole* kinetic energy of the Hubbard model. Physically, this is due to the fact that no matter how large  $U$  is, as long as it is finite, the lower-Hubbard band does not exactly correspond to the no double occupancy subspace and, to the leading order approximation of  $t/U$ , the correction  $2H_J$  in Eq.(5) originates from the *virtual* transitions of charge carriers to the doubly occupied states, which only vanishes at  $U = \infty$  or  $J = 0$ . Therefore, the kinetic energy at the level of the Hubbard model is different from the kinetic energy in the  $t - J$  model. Due to such a subtle difference, one has to distinguish the terminology of “kinetic energy driven vs. superexchange energy driven” at the level of the  $t - J$  model from “kinetic energy driven vs. potential energy driven” at the level of the Hubbard model to avoid confusion, which has been correctly noted [16] before.

In the optical sum rule, the kinetic energy of the Hubbard model is related to the total optical response in Eq.(1). According to the preceding discussion, the total optical weight of the Hubbard model is then composed of two contributions, namely the optical response within the subspace of no double occupancy and the optical response involving doubly occupied sites.

The first contribution is just the optical response of the  $t - J$  model, contributed by  $H_t$ . According to the optical sum rule, this contribution is related to kinetic energy of the  $t - J$  model in the following way

$$\int_0^\Omega \sigma_1(\omega) d\omega = \frac{\pi a^2}{2V} \langle -H_t \rangle. \quad (6)$$

Here an energy cutoff  $\Omega$  is a characteristic scale below which the charge response of the Hubbard model is equivalent to that of the  $t - J$  model.

The additional kinetic energy in Eq. (5) involving doubly occupied states should be determined by the optical weight between  $\Omega$  and  $\Lambda$  as given by

$$\begin{aligned} \int_{\Omega}^{\Lambda} \sigma_1(\omega) d\omega &= \frac{\pi a^2}{2V} \left\langle -2J \sum_{\langle i,j \rangle} \left( S_i \cdot S_j - \frac{1}{4} n_i n_j \right) \right\rangle \\ &= \frac{\pi a^2}{2V} \langle -2H_J \rangle \end{aligned} \quad (7)$$

which is thus related to the superexchange energy of the  $t - J$  model! Therefore, if we can determine the energy cutoff  $\Lambda$  and  $\Omega$ , we can read off both the kinetic energy and the superexchange energy of the  $t - J$  model from the optical data.

Recently, optical measurements in the cuprate  $Bi_2Sr_2CaCu_2O_8$  have revealed [19] a continuous spectral weight transfer from the high energy part to the low energy part of the in-plane optical conductivity with decreasing temperature, in both optimally doped and underdoped samples. An characteristic energy scale  $10^4 \text{ cm}^{-1}$  has been identified, which corresponds to the minimum of the in-plane optical conductivity in the experiment. Below and above it, the integrated optical conductivity behaves in opposite ways as a function of temperature. Namely, the spectral weight between  $10^4 \text{ cm}^{-1}$  to  $2 \times 10^4 \text{ cm}^{-1}$  transfers steadily to below  $10^4 \text{ cm}^{-1}$  with decreasing temperature, while the total spectral weight remains approximately conserved [19].

If we take  $10^4 \text{ cm}^{-1}$  as the energy cutoff  $\Omega$  for the  $t - J$  model described above and adopt  $2 \times 10^4 \text{ cm}^{-1}$  as  $\Lambda$ , below which reliable optical data is available [19], then the experimental result consistently indicates that, starting well above and persisting below  $T_c$ , the kinetic energy of the  $t - J$  model is continuously lowered whereas the superexchange energy is increased with decreasing temperature according to Eqs.(6) and (7). Such experimental results can be thus read off as evidence in support of the kinetic-energy-driven mechanism for *both* superconducting and pseudogap phases, so long as the  $t - J$  model is relevant to the cuprates with the energy cutoff of  $\Omega \sim 10^4 \text{ cm}^{-1}$  representing the characteristic energy scale for the intraband transitions within the no-double-occupancy subspace. Note that the value of the energy cutoff  $\Lambda$  of the Hubbard model is subjected to some uncertainty, but this may not matter much since the spectral weight approximately remains conserved as a function of temperature with  $\Lambda \gtrsim 2 \times 10^4 \text{ cm}^{-1}$  as stated above.

The steady increase of the superexchange energy with decreasing temperature seems at odd with the conventional understanding of the pseudogap as some kind of spin pairing gap forming, driven by the exchange energy of the  $t - J$  model. This indicates that the kinetic energy of the  $t - J$  model plays an important role in the formation of the pseudogap [28, 29]. In the next section, we shall investigate the detailed driving mechanisms for pseudogap phases in the  $t - J$  model based on two different mean-field theories and explore the underlying physics in comparison with experiment.

Finally we note that a closer examination on the experimental data shows that both kinetic and superexchange energies change more rapidly upon entering the superconducting state. This shows convincingly that the superconducting transition is kinetic energy driven while the exchange energy resists the transition. Also, we note that since the kinetic energy and superexchange energy evolve in opposite directions with temperature, the true superconducting condensation energy should be smaller than that estimated from the kinetic energy alone. Furthermore as the superconducting transition usually simultaneously involves the interlayer coherent hopping in the cuprates, one needs to further consider the  $c$ -axis conductivity in order to determine whether the intra or interlayer kinetic energy will predominantly “drive” the superconductivity [30, 31], if it is kinetic-energy-driven. Nevertheless, in the present work we shall be mainly interested in the formation of the pseudogap phase above  $T_c$ , where the out-of-plane physics is no longer as crucial, and one can thus mainly focus on the in-plane physics.

### III. TWO DISTINCT PSEUDOGAP PHASES BASED ON THE $t - J$ MODEL

#### A. Pseudogap phase in slave-boson RVB state

In the slave-boson formalism of the  $t - J$  model, the electron operator can be written as [20]

$$c_{i\sigma} = h_i^\dagger f_{i\sigma} \quad (8)$$

where  $h_i$  is a bosonic “holon” operator and  $f_{i\sigma}$  a fermionic “spinon” operator. They satisfy the no-double-occupancy constraint  $\sum_{\sigma} f_{i\sigma}^\dagger f_{i\sigma} + h_i^\dagger h_i = 1$  at each lattice site.

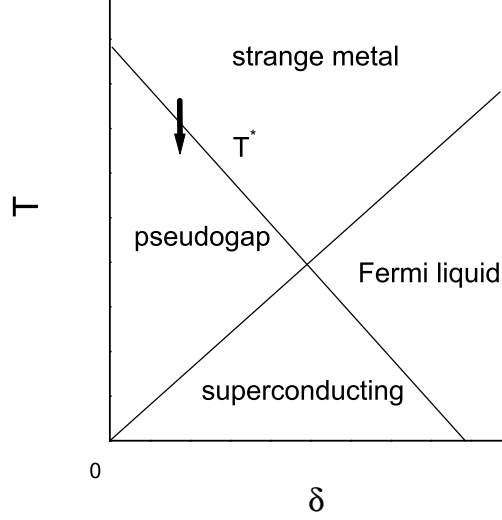


FIG. 1: The phase diagram of the slave-boson mean-field theory, which is divided into four regions by two lines representing the RVB pairing ( $\Delta^{\text{sb}} \neq 0$ ) and holon condensation ( $\langle h^\dagger \rangle \neq 0$ ), respectively. The pseudogap phase is defined by the RVB pairing of spinons below  $T^*$ , in the absence of the holon condensation. The latter determines the superconducting phase at low doping  $\delta$ . See Refs.[33] for details.

The pseudogap phase in the RVB mean-field theory based on this slave-boson formalism is characterized by a d-wave order parameter for the spinon pairing [21]

$$\begin{aligned} \Delta^{\text{sb}} &= \Delta_x^{\text{sb}} = -\Delta_y^{\text{sb}} \\ &= \frac{3}{8} \langle f_{i\uparrow} f_{i+x\downarrow} - f_{i\downarrow} f_{i+x\uparrow} \rangle \end{aligned} \quad (9)$$

which is finite at small doping below a characteristic temperature  $T^*$ . The pseudogap phase is defined in the temperature regime of  $T^* > T > T_c$ , where the superconducting transition temperature  $T_c$  is decided by the “holon” condensation ( $\langle h^\dagger \rangle \neq 0$ ) temperature in this mean-field description. The corresponding phase diagram [33] is schematically shown in Fig. 1.

Note that in the RVB mean-field theory [20, 21, 33], besides the RVB order parameter (9), one also needs to introduce the following order parameters  $\kappa = \kappa_x = \kappa_y = \frac{3}{8} \langle \sum_\sigma f_{i\sigma}^\dagger f_{i+x\sigma} \rangle$  and  $B = \langle b_i b_j^\dagger \rangle = \langle b_i^\dagger b_j \rangle$ . The detailed mean-field results concerning the pseudogap phase will be presented in Sec. IV.

## B. Pseudogap phase in the bosonic RVB state

### 1. Definition

In the phase-string formalism of the  $t - J$  model, the electron operator is decomposed as [22]

$$c_{i\sigma} = h_i^\dagger b_{i\sigma} e^{i\hat{\Theta}_{i\sigma}}. \quad (10)$$

In contrast to the slave-boson scheme (8), both the “holon”  $h_i$  and “spinon”  $b_{i\sigma}$  here are *bosonic* operators. In such a *bosonization* description, the fermionic commutation relations of  $c_{i\sigma}$ ’s can be restored by the phase-string factor  $e^{i\hat{\Theta}_{i\sigma}}$ .

As a distinctive feature of this decomposition, the definition of the phase-string factor is given by  $e^{i\hat{\Theta}_{i\sigma}} \equiv (-\sigma)^i e^{i\frac{1}{2}[\Phi_i^b - \sigma\Phi_i^h]}$ , where  $\Phi_i^b = \Phi_i^s - \Phi_i^0$ , with  $\Phi_i^s = \sum_{l \neq i} \theta_i(l) \sum_\alpha \alpha n_{l\alpha}^b$  and  $\Phi_i^0 = \sum_{l \neq i} \theta_i(l)$ , while  $\Phi_i^h = \sum_{l \neq i} \theta_i(l) n_l^h$ .

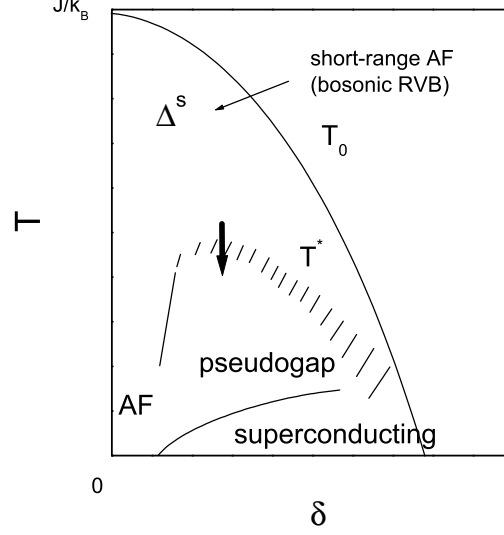


FIG. 2: The phase diagram in the b-RVB theory at low doping. From the top-down, the b-RVB pairing of spinons ( $\Delta^s \neq 0$ ) below  $T_0$  characterizing the short-range AF correlations. The pseudogap phase sets in below  $T^*$  when the bosonic holons experience the Bose condensation and thus the amplitude of the Cooper pairing forms ( $\Delta^0 \neq 0$ ). Eventually the superconducting phase is realized when the phase coherence is achieved. Note that the phase coherence factor in Eq.(11) is absent in the slave-boson RVB theory.

( $n_{i\alpha}^b$  and  $n_i^h$  are spinon and holon number operators. And  $\theta_i(l) \equiv \text{Im} \ln(z_i - z_l)$ , with  $z_l = x_l + iy_l$ .) It can be verified that the fermionic properties of  $c_{i\sigma}$ 's are ensured by such a phase factor under the no-double-occupancy constraint  $\sum_{\alpha} n_{i\alpha}^b + n_i^h = 1$ .

The pseudogap phase in the bosonic-RVB (b-RVB) state [23] based on the phase-string formalism is defined as follows. Firstly the d-wave superconducting order parameter  $\Delta^{SC}$  can be written as [32]

$$\Delta^{SC} = \Delta^0 e^{i\Phi^s} \quad (11)$$

where the pairing amplitude

$$\Delta^0 = \langle h^\dagger \rangle^2 \Delta^s \quad (12)$$

in which  $\Delta^s$  denotes the b-RVB order parameter, to be defined below. Thus, compared to the slave-boson mean-field theory, the superconducting order parameter has an extra phase factor  $e^{i\Phi^s}$  in Eq.(11). When the holons experience a Bose condensation, with  $\langle h^\dagger \rangle \neq 0$ , the state is not necessarily superconducting, if the phase  $\Phi^s$  still remains disordered.[28, 32]

Let us examine this from a “top-down” approach. We note that the b-RVB order parameter  $\Delta^s$  will first form at high temperature  $T_0$  ( $\sim J/k_B$  at small  $\delta$ ). Different from  $\Delta^{sb}$  in the slave-boson theory,  $\Delta^s$  here no longer corresponds to the opening of an energy gap. It characterizes short-range AF spin correlations according to  $\langle \vec{S}_i \cdot \vec{S}_j \rangle_{\text{NN}} = -3/8 |\Delta^s|^2$  and can persist over a wide range of temperatures and a finite doping regime as illustrated in Fig. 2.

Then the pseudogap phase in this framework is defined by [28]

$$\Delta^0 \neq 0 \quad (13)$$

The pairing amplitude  $\Delta^0$  becomes finite at a temperature  $T^*$  at which the bosonic holons are Bose condensed. On the other hand, the superconducting transition occurs at  $T_c$  when the phase coherence is realized [32] in Eq.(11), as the “spinon-vortices” in  $\Phi^s$  are bound together such that  $\Phi^s$  is cancelled out at large-distance scales. Note that the pseudogap phase between  $T^* > T > T_c$  is also called *spontaneous vortex phase* in Ref. [28] since free spinon-vortices are unbound in such a regime where the phase  $\Phi^s$  in Eq.(11) is disordered ( $T^*$  is denoted by  $T_v$  in Ref. [28]). It has been argued [28] that these free spinon-vortices will contribute to the Nernst effect observed experimentally.

## 2. Interplay between the kinetic and superexchange terms

Different from the standard slave-boson mean-field theory, the spinon and holon degrees of freedom in the b-RVB theory are intrinsically “entangled” together, which will be quite essential in the following discussion of the properties of the pseudogap phase. We shall first briefly discuss the basic theoretical structure of this model below.

The low-energy effective Hamiltonian  $H_{\text{string}} = H_h + H_s$  derived [23] from the phase-string formalism of the  $t - J$  model (with  $H_h$  and  $H_s$  corresponding to the hopping term  $H_t$  and the superexchange term  $H_J$ , respectively) under the bosonic RVB order parameter  $\Delta^s$  is given by

$$H_h = -t_h \sum_{\langle ij \rangle} \left( e^{iA_{ij}^s} \right) h_i^\dagger h_j + H.c. \quad (14)$$

$$H_s = -J_s \sum_{\langle ij \rangle \sigma} \left( e^{i\sigma A_{ij}^h} \right) b_{i\sigma}^\dagger b_{j-\sigma}^\dagger + H.c. \quad (15)$$

where  $t_h \sim t$  and  $J_s = J\Delta^s/2 \sim 0.5J$ , with  $\Delta^s = \sum_{\sigma} \left\langle e^{-i\sigma A_{ij}^h} b_{i\sigma} b_{j-\sigma} \right\rangle_{NN}$ .

An important feature of this effective model is a mutual entanglement between the charge and spin degrees of freedom as mediated by the gauge fields,  $A_{ij}^s$  and  $A_{ij}^h$ , which satisfy the following topological “constraints”

$$\sum_c A_{ij}^s = \pi \sum_{l \in c} (n_{l\uparrow}^b - n_{l\downarrow}^b) \quad (16)$$

and

$$\sum_c A_{ij}^h = \pi \sum_{l \in c} n_l^h \quad (17)$$

for a closed loop  $c$ . Thus, a “spinon” always sees a “holon” as a  $\pi$  fluxoid and a “holon” perceives a “spinon” as a  $\pm\pi$  fluxoid ( $\pm$  depends on the spin index).

In the pseudogap phase where the holons experience a Bose condensation,  $A_{ij}^h$  can be reduced to a vector field describing a uniform flux satisfying

$$\sum_{\square} A_{ij}^h \simeq \pi\delta. \quad (18)$$

Then  $H_s$  in (15) can be easily diagonalized.[23] In such a case, a characteristic spinon gap (thus a spin gap) will be opened up and the AF correlations will be suppressed at low energy (see Sec. IV). Since the majority of spinons remain in RVB pairing at low temperatures,  $A_{ij}^s$  will be substantially cancelled out in Eq.(16), which in turn is in favor of the holon condensation in  $H_h$  in a *self-consistent way*. So in the pseudogap phase, *the kinetic energy of the holons is expected to get improved at the expense of the AF correlations* according to the phase-string description.

On the other hand, in the “normal” state where the holon condensation is gone, the spinon gap will disappear and there will be *strong fluctuations* in  $A_{ij}^s$  due to unpaired  $\pm\pi$  fluxoid bound to *thermally excited* spinons in terms of Eq.(16). This will then lead to a great deal of frustrations on the holon part through  $H_h$ , again self-consistently, causing *holons lose phase coherence and behave incoherently*. In contrast to such a frustration of the kinetic energy of the charge carriers, strong AF correlations will be *restored* in  $H_s$  instead, where the gauge field  $A_{ij}^h$  can no longer treated as in Eq.(18), but rather as describing  $\pi$  fluxoids bound to randomly distributed holons according to Eq.(17), whose frustration effects on the AF correlations are found to be *minimal*, in contrast to the case of Eq.(18) in the pseudogap phase.

Therefore, one will find a distinctive interplay between the charge and spin degrees of freedom in the pseudogap state and “normal” state based on the framework of the b-RVB theory, characterized by Eqs.(14) and (15). Namely, the AF correlations and the kinetic energy are mutually repulsive to each other, whose competition becomes the driving force for the formation of the pseudogap phase at low temperatures. The detailed results will be presented in the following section.

## IV. RESULTS

### A. Exchange-energy-driven vs. kinetic-energy-driven

In the above we have introduced the definitions of pseudogap state in two different mean-field approaches in the  $t - J$  model. In this section, we explore and compare the driving mechanisms for such pseudogap states in the slave-

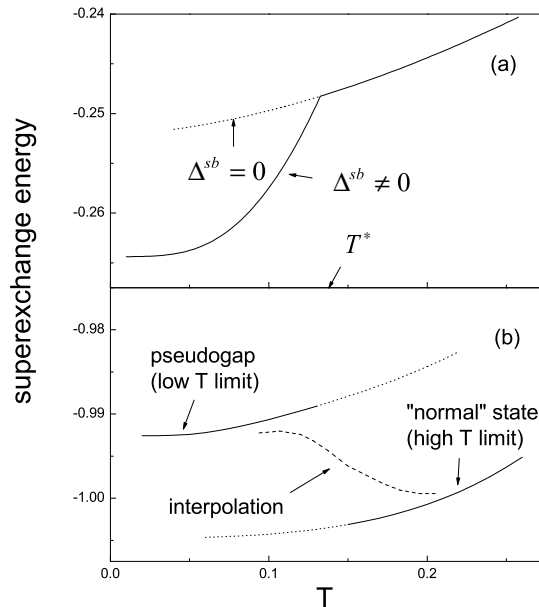


FIG. 3: The superexchange energies calculated in the slave-boson mean-field theory (a) and in the b-RVB theory (b). Two results show the *opposite* trends, indicating that while it is superexchange-energy-driven in the former, it is not in the latter. Note that the temperature in the horizontal axis is plotted in units of  $J$  in (a) and  $2J_s(\sim J)$  in (b).

boson and b-RVB descriptions, respectively, and show that two mechanisms are drastically distinct. Namely, one is exchange-energy-driven and the other is kinetic-energy-driven.

### 1. Superexchange energy

Let us consider the superexchange energy and examine the change of the superexchange energy during the formation of a pseudogap state according to the mean-field theories outlined in Sec. III.

Firstly let us focus on the pseudogap state in the slave-boson RVB theory, which is featured by the opening of the slave-boson RVB gap  $\Delta^{sb}$ . Since the origin of  $\Delta^{sb}$  comes entirely from  $H_J$ , the superexchange energy is expected to be gained in the pseudogap phase.

The calculation based on the mean-field theory outlined in Sec. III is standard and straightforward [21]. Fig. 3(a) shows the results calculated at  $\delta = 0.125$  in a  $32 \times 32$  square lattice. Clearly the superexchange energy is reduced with  $\Delta^{sb} \neq 0$  (solid curve) as compared to the state with  $\Delta^{sb} = 0$  (dotted curve) below the onset temperature  $T^*$ .

The result that the pseudogap phase is superexchange-energy-driven in the slave-boson theory is within the expectation as mathematically the fermionic spinon part closely resembles a BCS mean-field state where the attractive potential is obviously the driving force. Such a fact should remain true even if one includes the gauge fluctuations in both U(1) and SU(2) formalisms[33, 34]. Usually the gauge fluctuations will get suppressed in the pseudogap phase with the opening of the gap  $\Delta^{sb}$ . Such a competition between the pseudogap  $\Delta^{sb}$  and gauge fluctuations may quantitatively modify the superexchange energy, but not the driving mechanism itself.

Now let us consider the b-RVB state, in which the pseudogap phase is marked by the occurrence of the holon condensation. As discussed in Sec. III B, the corresponding effect of the holon condensation on the superexchange energy will be mediated through the topological gauge field  $A_{ij}^h$  in Eq.(15). Let us consider two extreme limits. In one limit, let all holons be condensed such that  $A_{ij}^h$  describes a uniform flux [Eq.(18)], which is deep in the pseudogap regime. In the opposite limit, all holons behave incoherently such that  $A_{ij}^h$  describes a *randomly distributed*  $\pi$  fluxoids on the lattice (of a total number  $N\delta$ ), which approximately represents the case of the high-temperature “normal” state. Fig. 3(b) illustrates the superexchange energy determined by the mean-field solution of  $H_s$  as a function of  $T$ , with  $A_{ij}^h$  being treated in the above-mentioned two limits, in a  $32 \times 32$  lattice. As shown by Fig. 3(b), it will always



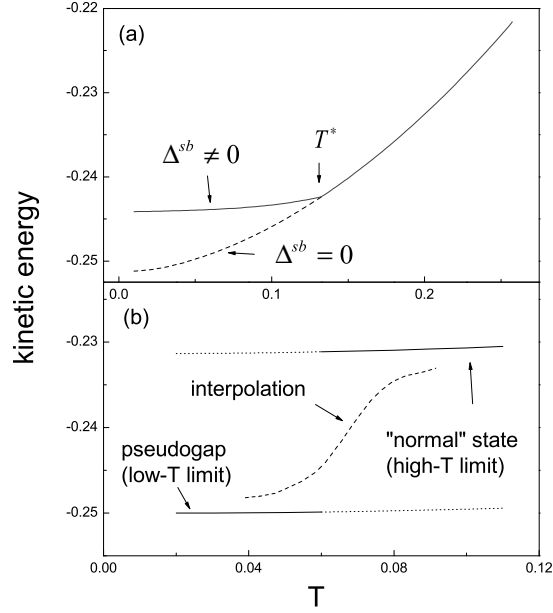


FIG. 4: The kinetic energies in the slave-boson mean-field theory (a) and b-RVB theory (b). The results are consistent with the superexchange energies given in Fig. 3, showing that the pseudogap phase is kinetic-energy-driven in the b-RVB theory, whereas it is superexchange-energy-driven in the slave-boson mean-field theory. Note that  $T$  axis is in units of  $J$  in (a) while in units of  $t_h$  in (b).

cost the superexchange energy going into the pseudogap state from the high- $T$  “normal” state.

Note that in the temperature range between these two limits,  $A_{ij}^h$  itself should behave more complicated than the above simple-minded treatments, which in general involves the holon dynamics. It is usually difficult to determine the true superexchange energy as a function of temperature in a self-consistent way, whose realistic behavior is sketched by a long dashed curve in Fig. 3(b). Nevertheless, in the two opposite limits at low- and high-temperatures the results present in Fig. 3(b) should be reliable, which unambiguously indicate that the pseudogap state is formed at the expense of the superexchange energy in the b-RVB theory, in contrast to the superexchange-energy-driven picture for the slave-boson mean-field theory shown in Fig. 3(a).

## 2. Kinetic energies

Consistent with the divergent behaviors of the superexchange energies in two theories, the kinetic energies for the two RVB mean-field states also show opposite trends upon entering the pseudogap phases.

First of all, the kinetic energy in the slave-boson mean-field state can be also straightforwardly calculated as shown in Fig. 4(a). Obviously the kinetic energy is lost with the opening the RVB gap  $\Delta^{sb}$ . Thus, in combination with Fig. 3(a), it is established that the pseudogap phase in the slave-boson RVB theory is indeed *superexchange-energy-driven*.

Next, we consider the kinetic energy based on  $H_h$  in the b-RVB theory. Here  $H_h$  describes that free bosonic holons hop in the presence of a gauge field  $A_{ij}^s$ , which depicts  $\pm\pi$  flux-tubes bound to spinons. At low temperatures, when spinons are well paired in the RVB state,  $A_{ij}^s$  will get suppressed. In this case, the bosonic holons will experience a Bose condensation. This is the pseudogap phase defined in the b-RVB state as discussed in Sec. III B. Here a spin gap is opened up in the spin excitation spectrum such that to break up an RVB pair or equivalently a vortex-anti-vortex bound pair in  $A_{ij}^s$  will cost an energy  $E_g$  (see Fig. 8 below). It means that the fluctuations in  $A_{ij}^s$  will be suppressed at low temperatures, which then enforces the holon condensation in  $H_h$  in a self-consistent fashion. In the opposite limit, when a lot of free spinon excitations are created at high temperatures, strong fluctuations of  $A_{ij}^s$  due to the free  $\pm\pi$  flux-tubes bound to excited spinons will destroy the bosonic holons' phase coherence and cause them behave incoherent.

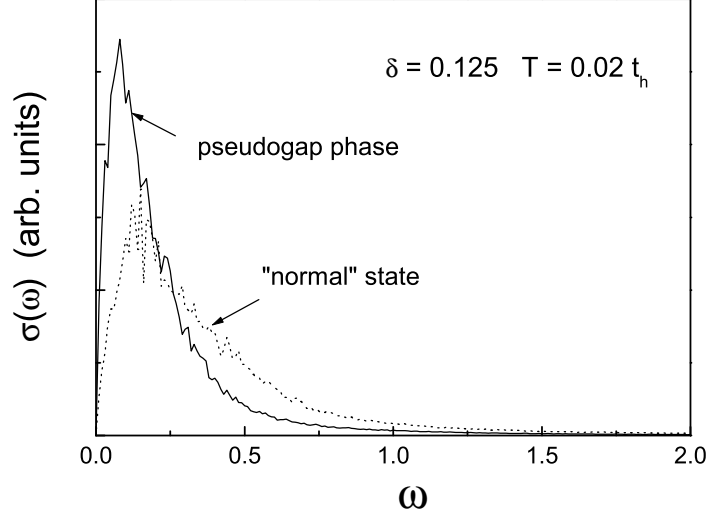


FIG. 5: The optical conductivity in the b-RVB theory calculated in the pseudogap phase and “normal” phase as defined in the text. The spectral weight shifts towards the low energies as it enters the pseudogap phase. Here the  $\omega$ -axis is plotted in units of  $t_h$ .

Thus, we can calculate the kinetic energy based on  $H_h$  in such two extreme limits, similar to the preceding discussion of the superexchange term. In the deep pseudogap limit, one may simply treat  $A_{ij}^s = 0$  and the holons as non-interacting bosons. In the high-temperature “normal” state, one can treat  $A_{ij}^s$  as describing  $\pm\pi$  flux-tubes bound to free spinons, which are randomly distributed on lattice to simulate those excited from the RVB background with a number  $n_{\text{spinon}}^{\text{free}}(T)$ . Generally  $n_{\text{spinon}}^{\text{free}}(T)$  should increase with the temperature. For our purpose, we can define a prototype “normal” state with  $n_{\text{spinon}}^{\text{free}}$  fixed at  $2\delta N$  (note that  $n_{\text{spinon}}^{\text{free}} \sim \delta N$  at  $T = T_c$  [23, 32]), and calculate the average kinetic energy  $\langle H_h \rangle$  as a function of temperature.

Fig. 4(b) shows the results. The kinetic energy  $\langle H_h \rangle$  does decrease with the decrease of  $n_{\text{spinon}}^{\text{free}}$ , which means that with the decrease of the temperature, the kinetic energy of holons will get continuously improved due to the suppression of the fluctuations in  $A_{ij}^s$ . Again the realistic case will be some kind of interpolation between the solid curves shown in Fig. 4(b). But it does not change the general trend that the kinetic energy will be gained by entering the pseudogap phase, *i.e.*, a kinetic-energy-driven mechanism, which is consistent with the loss of the superexchange energy discussed earlier on.

Finally, we have computed the optical conductivity in the b-RVB theory. Based on the same approximation in dealing with  $H_h$  above, the optical conductivity is obtained in Fig. 5 for two cases of the pseudogap and “normal” states with  $n_{\text{spinon}}^{\text{free}} \sim \delta N$  and  $n_{\text{spinon}}^{\text{free}} \sim 2\delta N$ , respectively. It shows that the low-energy spectral weight does increase in the pseudogap phase as compared to the normal state, in consistency with the kinetic energy behavior.

## B. Spin-spin correlations

The sharp contrast between the qualitative behaviors of the superexchange and kinetic energies in two mean-field theories is quite remarkable, as they are supposed to describe the same  $t - J$  model. In the following, we analyze the detailed spin-spin correlations in order to understand the physics underlying such distinctions.

### 1. Uniform spin susceptibility

The uniform spin susceptibility  $\chi_u$  in the cuprates has generally exhibited a suppression at low temperatures in the underdoped phase. This behavior has served as one [35] of the main experimental evidence for the existence of a

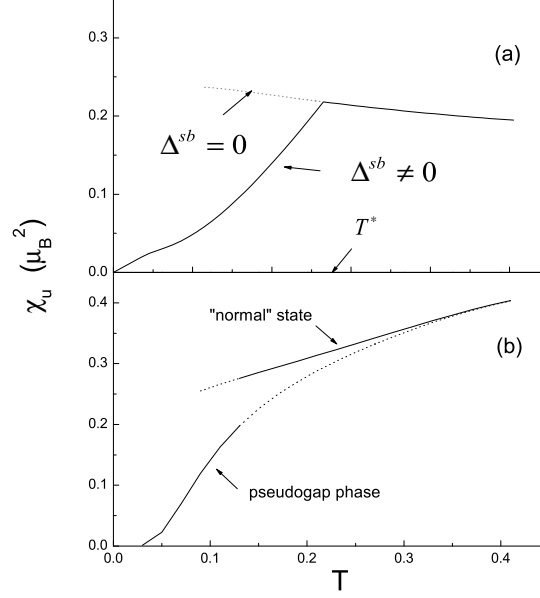


FIG. 6: A comparison of the uniform spin susceptibilities in the slave-boson mean-field theory (a) and b-RVB theory (b). Both show a suppression at low temperatures, indicating the opening up of a spin gap near momentum  $(0,0)$ . The  $T$ -axis is scaled with  $J$  in (a) and  $2J_s$  in (b).

pseudogap above  $T_c$ .

In the slave-boson RVB theory, the opening of the RVB gap  $\Delta^{sb}$  will naturally result in the suppression of  $\chi_u$  at low temperature as shown in Fig. 6(a). Similarly, in the b-RVB state, the uniform spin susceptibility  $\chi_u$  also shows a continuous reduction at low temperatures, as given in Fig. 6(b), where the curves calculated in the two limits of the pseudogap and “normal” states (corresponding to Fig. 3(b)) are presented for comparison.

Here we see that the pseudogap behavior in the uniform spin susceptibility is not very sensitive to the detailed mechanisms and the general trend remains essentially the same. This implies that the density of spin states near momentum  $(0,0)$  is indeed universally suppressed in both cases. However, the situation will become quite different when we consider spin-spin correlations near the AF momentum  $(\pi, \pi)$  below.

## 2. Equal-time spin-spin correlations

The superexchange energy is related to the equal-time NN spin-spin correlations in the  $t - J$  model. In the slave-boson RVB mean-field state, the equal-time the spin-spin correlation function is shown in Fig. 7(a). An enhancement of the NN spin correlations is the direct reason that the superexchange energy is gained in the pseudogap state. It is noted that the overall AF correlations are quite weak for both the normal and pseudogap states in Fig. 7(a), which can be visibly strengthened after the Gutzwiller projection is applied.

Similarly, one can compute the equal-time spin correlation function in the b-RVB description. The results for the pseudogap and normal states are presented in Fig. 7(b), respectively, in the two limits shown in Fig. 3(b), indicates that the spin-spin correlations are clearly suppressed in the pseudogap state, which is responsible for the increase of the superexchange energy in Fig. 3(b).

At this step, we can see that the main distinction between two pseudogap states is closely related to the AF correlations. In the slave-boson mean-field state, the short-range AF correlations are rather weak in the normal state, and by opening an RVB gap, the spin-spin correlations near  $(\pi, \pi)$  will get improved (note that the comparison is made at the *same* temperature by extrapolation to  $T = 0$ ). This general trend will not be altered even if one introduces the Gutzwiller projection, although the overall AF correlations can be enhanced by the projection for *both* cases.

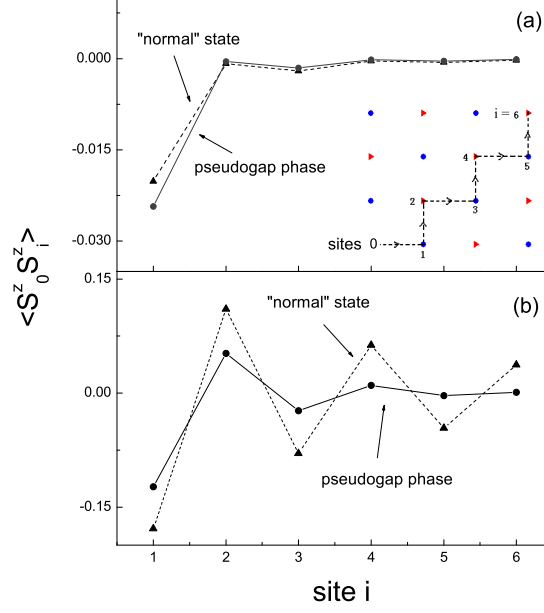


FIG. 7: Equal-time spin-spin correlation function in the slave-boson theory (a) and b-RVB theory (b) in both the pseudogap and "normal" states. All results here are compared at  $T = 0$ .

In contrast, the AF correlations in the normal phase of the b-RVB state are already quite strong, and are always suppressed by entering the pseudogap phase, thus leading to the superexchange-energy loss.

So the change of the AF correlations will hold the key to understanding the mechanisms for the above pseudogap phases. Generally speaking, weak AF correlations in the spin background favor the hopping of the holes. This is the reason why the kinetic energy in the slave-boson mean-field state is better in the normal state, whereas is reduced as the RVB gap  $\Delta^{\text{sb}}$  opens up with the improved short-range AF correlations. On the other hand, the AF correlations are much stronger in the normal phase of the b-RVB state, which is not in favor of the kinetic energy. So the holons can only hop incoherently under the influence of the randomly distributed  $\pm\pi$  fluxoids via  $A^s$  in the phase-string description. In the pseudogap phase of the b-RVB state, the hopping of the holons becomes coherent and the holons are condensed with better kinetic energies, at the expenses of the AF correlations which become gapped (Fig. 8 below).

In the following, the change in the AF oscillations of  $\langle S_i^z S_j^z \rangle$  can be further analyzed in terms of the weight transfer in the dynamic susceptibility function  $\text{Im} \chi^{zz}(\vec{q}, \omega)$  at different energies for a fixed  $\vec{Q}_{\text{AF}} = (\pi, \pi)$ , according to the Fourier transformation of Eq.(2).

### 3. Dynamic spin susceptibility near $(\pi, \pi)$

In the pseudogap phase based on the bosonic RVB description, the equal-time AF correlations have been shown to be suppressed. In the following, we further investigate how such a suppression is exhibited as a function of the frequency  $\omega$  near the AF momentum  $(\pi, \pi)$ .

Fig. 8 shows  $\text{Im} \chi^{zz}(\vec{q}, \omega)$  at  $\vec{Q}_{\text{AF}} = (\pi, \pi)$  in the two extreme limits of the pseudogap and "normal" states shown in Fig. 3(b). Note that the temperature is set at zero for both cases, just for convenience. In the pseudogap phase, a resonance-peak at  $\vec{Q}_{\text{AF}}$  emerges around  $E_g \sim 0.5(2J_s)$  at  $\delta = 0.125$ . In the previous work, [23] such a sharp-peak structure has been used to explain the so-called 41 meV resonance-like peak observed by the inelastic neutron-scattering in the optimal-doped YBCO compound [24], where  $T^*$  seems to coincide with  $T_c$ . A broader peak feature has been also found [25] in the underdoped YBCO compounds at  $T_c < T < T^*$ , and the present theory provides a natural description. Note that the sharpness of the peak in Fig. 8 is due to the artifact in treating the

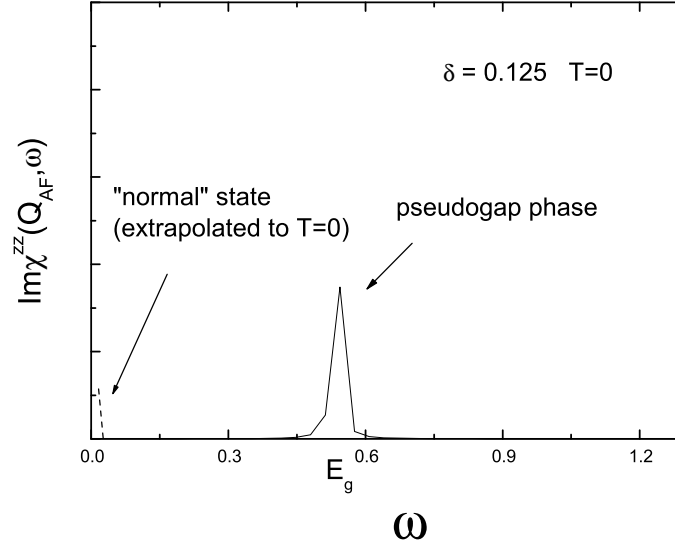


FIG. 8: Dynamic spin susceptibility obtained in the b-RVB theory at  $Q_{AF} = (\pi, \pi)$ . A resonance-like peak is found at an energy  $E_g \sim \delta J$  in the pseudogap phase, which disappears in the high- $T$  “normal” state where the weight in  $\text{Im}\chi(\omega)$  is shifted to  $\omega \sim 0$  when extrapolated to  $T = 0$ . The  $\omega$ -axis is in units of  $2J_s \sim J$ .

gauge field  $A_{ij}^h$  by assuming the holons are all in an ideal Bose condensation. It can be easily broadened once the density fluctuations of holons are considered.

The resonance-like peak around  $E_g$  disappears in Fig. 8 in the “normal” state when the holon coherence is gone and the holons behave like incoherent objects, such that  $A_{ij}^h$  can be treated as describing randomly distributed  $\pi$  flux-tubes as discussed in Sec. III B. The dashed curve shows the corresponding result artificially extrapolated to  $T = 0$ , with the remaining spectral weight at  $\vec{Q}_{AF}$  shifting down to the low frequency  $\omega \sim 0$ . This is consistent with the fact that the AF correlations will be enhanced in the “normal” state.

We can further study the AF correlations near  $\omega \sim 0$  by calculating  $\text{Im}\chi^{zz}(\vec{q}, \omega)/\omega$  at  $\vec{Q}_{AF}$  and  $\omega \rightarrow 0$ . Note that such a quantity is related to the NMR spin relaxation rate  $1/T_1T$  for  $^{63}\text{Cu}$  nuclear spins (a  $\vec{q}$ -dependent hyperfine coupling factor is neglected here for simplicity). The results for the two extreme limits considered before are shown in Fig. 9: the main panel is for the “normal” state case, which demonstrates a non-Korringa behavior often observed [36] in the cuprates due to strong AF correlations near  $\vec{Q}_{AF}$  and  $\omega \sim 0$ . By contrast, a spin gap behavior of  $1/T_1T$  also seen in experiment [35] is indeed exhibited in the pseudogap state as shown in the inset of Fig. 9. Both are qualitatively consistent with the experimental measurements in the cuprate superconductors.

So far we have only considered the dynamic spin susceptibility function based on the b-RVB theory. Note that the AF correlations are generally quite weak in the slave-boson mean-field theory [see Fig. 7(a)] and there are not much features near  $\vec{Q}_{AF}$  to give rise to the experimentally interested properties like  $1/T_1T$ , etc., at the mean-field level. One has really to go beyond the mean-field approximation here. For example, a resonance-like peak structure around  $\vec{Q}_{AF}$  has been obtained in the superconducting phase after a modified random-phase-approximation approach [37]. This is beyond the scope of the present work. Nevertheless, the conclusion that the superexchange energy will be *gained* by the opening of the pseudogap  $\Delta^{\text{sb}}$  should still hold true, as discussed in Sec. IV A, as responsible by an enhancement of the equal-time (frequency-integrated) spin correlations at a large momentum around  $(\pi, \pi)$  [opposed to the suppression of the uniform susceptibility near  $(0, 0)$ ].

## V. DISCUSSION AND CONCLUSIONS

In this paper, we have shown that the recent optical measurements of the cuprates have clearly demonstrated that both the pseudogap and superconducting phases are driven by the kinetic energy within the  $t - J$  model description,

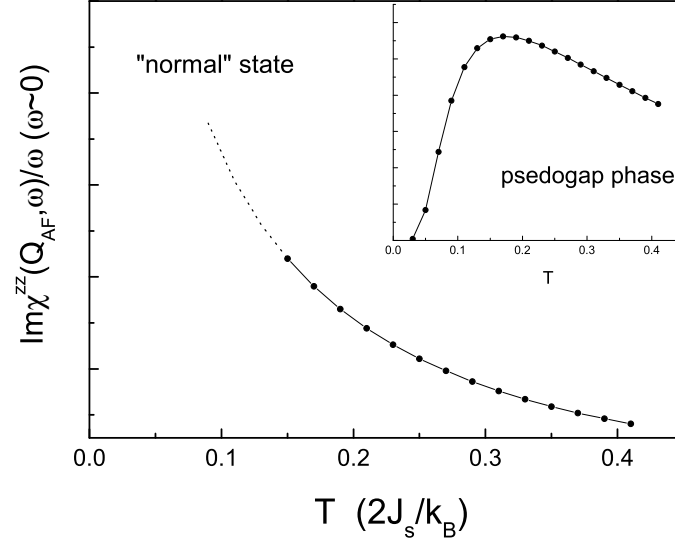


FIG. 9:  $\text{Im}\chi(\vec{Q}_{\text{AF}}, \omega)/\omega$  at  $\omega \rightarrow 0$  is shown as a function of  $T$  in the b-RVB theory. Such a quantity is approximately related to the spin relaxation rate in NMR measurement.

based on a general consideration of the optical sum rule in the Hubbard model and its relation to the  $t - J$  model. Under such an analysis, by entering the pseudogap phase, the superexchange energy of the  $t - J$  model should get suppressed instead.

Then, we have examined two pseudogap phases obtained in the slave-boson RVB and b-RVB mean-field states of the  $t - J$  model. Although the uniform spin susceptibility is universally suppressed in both cases, which is consistent with experiment, the underlying driving mechanisms for the pseudogap phases are found to be precisely opposite. Namely, it is superexchange-energy-driven in the slave-boson RVB theory as opposed to the kinetic-energy-driven in the b-RVB theory. If the above general consideration based on the optical sum rules is correct, then we conclude that the superexchange-energy-driven mechanism in the slave-boson RVB state is not supported experimentally.

The distinction between the two cases is very basic and physically revealing. It can be traced back to the central issue concerning the AF correlations. In the high- $T$  phase ("normal" state) of the slave-boson mean-field state, the AF correlations are relatively quite weak, which is fairly favorable to the kinetic energy of holes as the latter can easily hop on the uniform RVB background. In the low- $T$  phase (pseudogap state), an RVB pairing of spinons emerges, which improves the superexchange energy as well as the short-range AF correlations (or more precisely, the spin correlations at large-momenta), whereas the holes become less easy to hop around with the increasing kinetic energy.

By contrast, there already exist strong AF correlations in the high- $T$  phase ("normal" state) of the b-RVB state, characterized by the b-RVB order parameter  $\Delta^s$  which can persist up to  $T \sim J/k_B \sim 1,500$  K at low doping. In this regime, the kinetic energy of holes is actually strongly suppressed and the holons behave like incoherent objects moving in a short-range AF correlated spin background. This is quite different from the above slave-boson RVB state. Only in the low- $T$  pseudogap phase can the phase coherence of the holons be restored with gaining the kinetic energy. It occurs at the expense of the low-energy AF correlations, or the superexchange energy, and thus is entirely kinetic-energy-driven.

Mathematically, the whole interplay is straightforward in the slave-boson mean-field theory. However, the interplay in the b-RVB theory is different: due to the presence of strong AF correlations, the low-energy effective theory is no longer a mean-field one by nature. The charge and spin degrees of freedom are generally *entangled* together by a mutual Chern-Simons-type gauge structure, reflecting the phase string effect as described in Eqs.(14) and (15). Thus the pseudogap and "normal" states differ not simply by some mean-field order parameters, as in the slave-boson RVB states.

Here strong AF correlations will influence the hopping of holons through the topological gauge field  $A_{ij}^s$ , as if each excited spinon is a  $\pi$  fluxoid, which severely frustrate the phase coherence of the holons. On the other hand, when

the bosonic holons recover their phase coherence and are Bose condensed at low- $T$ , they will affect the spinon degrees of freedom drastically through the topological gauge field  $A_{ij}^h$  in Eq.(15), going from a random distributed  $\pi$  fluxoids bound to the incoherent holons at high- $T$  to the uniform flux given in Eq.(18) in the holon condensed (pseudogap) phase. The AF correlations at low-energy is subsequently suppressed (gapped) in the pseudogap phase relative to the high- $T$  phase, pushing the weight up towards a higher energy  $E_g$  to form a “resonance-like” peak as shown in Fig. 8 and to result in the reduction of the NMR spin relaxation rate in Fig.9. Self-consistently, the opening of the spinon gap at low-energies will substantially reduce the fluctuations of  $A_{ij}^s$  in the hopping term and improve the kinetic energy as shown in Fig. 4(b) as well as the low-energy optical conductivity in Fig. 5, which further strengthens the holon Bose condensation, and thus the pseudogap phase.

### Acknowledgments

We acknowledge helpful discussions with W. Q. Chen and X. L. Qi. This work is supported by the grants of NSFC, the grant no. 104008 and SRFDP from MOE of China.

- 
- [1] For a review, see, T. Timusk and B. Statt, Rep. Prog. Phys. **62**, 61 (1999).
  - [2] P. W. Anderson, Science **235**, 1196 (1987).
  - [3] G. Baskaran, Z. Zou, P. W. Anderson, Solid State Comm. **63**, 973 (1987).
  - [4] P. W. Anderson, P. A. Lee, M. Randeria, T. M. Rice, N. Trivedi, F. C. Zhang, cond-mat/0311467.
  - [5] V. J. Emery and S. A. Kivelson, Nature **374**, 434 (1995).
  - [6] J. Orenstein and A. J. Millis, Science **288**, 468 (2000).
  - [7] S. Alexandrov and N. F. Mott, *High Temperature Superconductors and Other Superfluids* (Taylor and Francis, London, 1994).
  - [8] S. Chakravarty, R. B. Laughlin, D. K. Morr and C. Nayak, Phys. Rev. B **63**, 094503 (2001).
  - [9] P. W. Anderson, Science **279**, 1196 (1998); Physica C **341-348**, 9 (2000).
  - [10] J. E. Hirsch, Physica C **199**, 305 (1992).
  - [11] D. J. Scalapino and S. R. White, Phys. Rev. B **58**, 8222 (1998).
  - [12] E. Demler and S. C. Zhang, Nature **396**, 733 (1998).
  - [13] J. E. Hirsch, Science **295**, 2226 (2002).
  - [14] M. R. Norman and C. Pépin, Phys. Rev. B **66**, 100506 (2002).
  - [15] T. K. Kopeć, Phys. Rev. B **67**, 014520 (2003).
  - [16] S. Chakravarty, H.Y. Kee and E. Abrahams, Phys. Rev. B **67**, 100504(R) (2003).
  - [17] C. C. Homes and S. V. Dordevic, D.A. Bonn, R. Liang, W.N. Hardy, Phys. Rev. B **69**, 024514 (2004).
  - [18] J. E. Hirsch and F. Marciglio, Phys. Rev. B **62**, 15131 (2000).
  - [19] H. J. A. Molegraaf, C. Presura, D. van der Marel, P. H. Kes, and M. Li, Science **295**, 2239 (2002).
  - [20] Z. Zou and P. W. Anderson, Phys. Rev. B **37**, 627 (1988).
  - [21] G. Kotliar and J. Liu, Phys. Rev. B **38**, 5142 (1988).
  - [22] Z.Y. Weng, D.N. Sheng, Y.C. Chen, and C. S. Ting, Phys. Rev. B **55**, 3894 (1997).
  - [23] Z. Y. Weng, D. N. Sheng and C. S. Ting, Phys. Rev. Lett. **80**, 5401 (1998); Phys. Rev. B **59**, 8943 (1999).
  - [24] H. F. Fong, B. Keimer, P. W. Anderson, D. Reznik, F. Dogan and I. A. Aksay, Phys. Rev. Lett. **75**, 316 (1995).
  - [25] H. F. Hong, P. Bourges, Y. Sidis, L. P. Regnault, J. Bossy, A. Ivanov, D. L. Milius, I. A. Aksay and B. Keimer, Phys. Rev. B **61**, 14773 (2000).
  - [26] P. Dai, H. A. Mook, S. M. Hayden, G. Aeppli, T. G. Perring, R. D. Hunt, and F. Doan, Science **284**, 1344 (1999).
  - [27] G. Baskaran, Z. Zou, and P. W. Anderson, Solid State Commun. **63**, 973 (1987).
  - [28] Z. Y. Weng and V. N. Muthukumar, Phys. Rev. B **66**, 094509 (2002).
  - [29] W. Rantner and X. G. Wen, Phys. Rev. B **66**, 144501 (2002).
  - [30] P. W. Anderson, *The Theory of Superconductivity in the High  $T_c$  Cuprates*, (Princeton Univ. Press, Princeton, 1997).
  - [31] S. Chakravarty, H. Y. Kee, and E. Abrahams, Phys. Rev. Lett. **82**, 2366 (1999).
  - [32] V. N. Muthukumar and Z. Y. Weng, Phys. Rev. B **65**, 174511 (2002).
  - [33] P. A. Lee and N. Nagaosa, Phys. Rev. B **46**, 5621 (1992).
  - [34] X. G. Wen and P. A. Lee, Phys. Rev. Lett. **76**, 503 (1996); P.A. Lee, N. Nagaosa, T.K. Ng, and X.-G. Wen, Phys. Rev. B **57**, 6003 (1998).
  - [35] A. J. Millis and H. Monien, Phys. Rev. Lett. **70**, 2810 (1993).
  - [36] R. E. Walstedt, B. S. Shastry, and S-W. Cheong, Phys. Rev. Lett. **72**, 3610 (1994), and references therein.
  - [37] J. Brinckmann and P. A. Lee, Phys. Rev. Lett. **82**, 2915 (1999).